The diffraction of sound pulses
I. Diffraction by a semi-infinite plane

By F. G. Friedlander

(*Communicated by G. I. Taylor, F.R.S.—Received* 29 *February* 1940)

This paper contains the results of some calculations which show the changes undergone by a sound pulse when it is diffracted by an infinite screen or wall with a straight edge. The incident pulse is travelling in such a manner that its wave front is parallel to the plane of the wall and the motion is assumed to be two-dimensional. The calculations are carried out for a certain pulse in which the pressure rises instantaneously and then decays exponentially, and—in less detail—for several other types of incident pulse. The pressure changes in the geometrical shadow and near its boundary are investigated, as well as the pressure at points on the screen itself. A remarkable feature is the propagation of the initial pressure discontinuity along the boundary of the geometrical shadow as an instantaneous pressure discontinuity across this boundary. The problem could be treated by the application of Fourier transforms to Sommerfeld's well-known solution of the diffraction of simple harmonic waves by a straight edge, but the analysis utilized in this paper offers many advantages, particularly when the incident pulse starts with a discontinuous pressure rise. It is also shown that, although the two solutions of the problem treated in this paper (which are due to Sommerfeld and Lamb respectively) differ in form, one can be obtained from the other by a suitable transformation.

Introduction

The diffraction of a simple harmonic wave train by a straight-edged semi-infinite screen, and by an infinite wedge, was originally discussed by Sommerfeld (1895). In a later paper Sommerfeld (1901) extended his analysis to the diffraction of pulses and treated the case of a 'rectangular pulse' in detail. The analysis of Sommerfeld's first paper was simplified by Lamb (1906), who also dealt with the reflexion of simple harmonic waves by a convex parabolic cylinder, and by a paraboloid. Lamb then applied his method to the diffraction of a pulse by a semi-infinite screen. His result differs in form from that given by Sommerfeld, but it will be shown in this paper that it can be transformed in such a manner that Sommerfeld's formulae are obtained.

Although the cases of pulse diffraction and of 'wave' diffraction (the latter refers to infinite trains of simple harmonic waves) are analogous, they differ in several respects. The equation governing the propagation of

pulses, i.e. the sound equation, is of the hyperbolic type; that governing wave diffraction is of the elliptic type. The functions satisfying these equations behave quite differently.* In wave diffraction, interference between 'elementary waves' produces certain alternating maxima and minima of intensity, which give rise to the diffraction bands well known in optics. Nothing of this nature must be expected in the case of a pulse: interference occurs because of the persistence and the periodicity of a wave train.

It is well known that every pulse can be thought of as made up by the superposition of simple harmonic waves; in other words, that it is possible to extend results about simple harmonic waves to the case of a pulse by applying a Fourier transform. When using this method during some preliminary calculations it was found that, if the integrals involved had to be evaluated numerically, the work tended to become very laborious and inaccurate. The formulae which were finally used were of a simpler type and much more suitable for numerical evaluation. They indicate very clearly the superiority of direct solutions of pulse diffraction problems over those obtained by Fourier transforms, particularly when the incident pulse has a well-defined wave front. It is usually difficult to obtain the general characteristics of the diffracted pulse from solutions of the Fourier transform type. For example, it requires considerable mathematical ingenuity to deduce the shape of the wave front in the shadow of an obstacle from such a solution, while it can be obtained from the direct solution by inspection. These difficulties are, on the whole, due to the fact that the Fourier transform provides the link between the solutions of partial differential equations of different types satisfied by different classes of functions; a point which has been mentioned above.

There are very few general methods available for obtaining the solutions of pulse diffraction problems. Similarly, approximate methods have only been little developed. Most of the approximate methods used in the treatment of wave diffraction apply only to limited frequency ranges and thus cannot be generalized by the application of a Fourier transform. Huygens's principle, in the form given to it by Kirchhoff,† can be applied to pulse diffraction.‡ But it seems unavoidable to ignore reflected waves in the application of this principle; this is equivalent to assuming the diffracting obstacles to be absorbing, an assumption which is quite legitimate

* This is discussed, for example, by Hadamard in *Le problème de Cauchy* (Paris, 1932), pp. 37 *et seq.*

† See, for example, Lamb, *Hydrodynamics*, 6th ed. p. 501.

‡ I am indebted to Dr E. C. Bullard for pointing out this possibility.

in optics, but of doubtful validity in the theory of sound. As a material usually only absorbs sound whose wave-length (or some equivalent dimension) is a small fraction of the thickness of the material, Huygens's principle —together with the assumptions made in approximate calculations—must be applied with great caution.

The solutions of pulse diffraction problems which are known thus become important as an indication of the general character of pulse diffraction. It is hoped that the results given in this paper will serve, apart from their intrinsic interest, to give some general indications of this kind.

Mathematical solution

Choose the co-ordinate system so that the z-axis coincides with the edge of the wall, which occupies the positive part of the x-z-plane. The motion will then depend only on x, y, and the time t. It is convenient to introduce parabolic co-ordinates, defined by

$$x+iy=(\xi+i\eta)^2 \quad \text{or} \quad \left.\begin{aligned}\xi^2-\eta^2&=x,\\ 2\xi\eta&=y.\end{aligned}\right\} \tag{1}$$

Thus the x-y-plane is transformed into the upper half of the ξ-η-plane, the positive half of the x-axis (which is the intersection of the wall with the x-y-plane) being transformed into the whole of the ξ-axis. The curves $\xi=\text{const.}$, $\eta=\text{const.}$ respectively are systems of confocal parabolas having the origin as common focus and the x-axis as common axis (see figure 1). The boundary condition expressing reflexion at the wall is

$$\frac{\partial\Phi}{\partial y}=0 \quad (y=0, x\geqslant 0) \qquad \text{or} \qquad \frac{\partial\Phi}{\partial\eta}=0 \quad (\eta=0) \tag{2}$$

(see Lamb 1906), where Φ is the velocity potential. Thus in the transformed plane the whole of the ξ-axis appears as a reflector.

The velocity potential must satisfy the sound equation

$$\frac{\partial^2\Phi}{\partial x^2}+\frac{\partial^2\Phi}{\partial y^2}=\frac{1}{c^2}\frac{\partial^2\Phi}{\partial t^2}, \tag{3}$$

where c is the velocity of sound. It is assumed that the motion is sufficiently small for this equation to hold. The incident pulse can then be represented by the velocity potential

$$F(ct+y) \quad \text{or} \quad F(ct+2\xi\eta). \tag{4}$$

Lamb (1910) showed that the solution which can be made to satisfy the boundary conditions at the half-plane and at infinity is

$$\Phi = \tfrac{1}{2}F(ct+2\xi\eta)+\tfrac{1}{2}F(ct-2\xi\eta)+\int_0^{\xi+\eta} f(ct+2\xi\eta-\zeta^2)\,d\zeta + \int_0^{\xi-\eta} f(ct-2\xi\eta-\zeta^2)\,d\zeta \qquad (5)$$

(see Lamb 1910), where the function f, which appears under the integral sign, is unspecified. It is easily verified by differentiation that (5) satisfies the equation (3). It also fulfils the boundary condition (2). For we have

$$\frac{\partial\Phi}{\partial\eta} = \xi\{F'(ct+2\xi\eta)-F'(ct-2\xi\eta)\} + \int_0^{\xi+\eta} 2\xi f'(ct+2\xi\eta-\zeta^2)\,d\zeta - \int_0^{\xi-\eta} 2\xi f'(ct-2\xi\eta-\zeta^2)\,d\zeta,$$

which vanishes when $\eta = 0$. That this must be so is also apparent from the form of (5) which consists of two groups of terms, one of which is the 'image' of the other with respect to the ξ-axis.

To determine the function f, Lamb (1906) uses the additional condition that in the region of great negative x the motion must closely approximate to the incident wave, i.e. as

$$x \to -\infty, \quad \Phi \to F(ct+y). \qquad (6)$$

It follows from (1) that as

$$x \to -\infty, \quad \xi+\eta \to +\infty, \quad \xi-\eta \to -\infty,$$

hence (6) becomes, substituting from (5),

$$F(ct+2\xi\eta) = \tfrac{1}{2}F(ct+2\xi\eta)+\tfrac{1}{2}F(ct-2\xi\eta) + \int_0^{\infty} f(ct+2\xi\eta-\zeta^2)\,d\zeta - \int_0^{\infty} f(ct-2\xi\eta-\zeta^2)\,d\zeta.$$

For this to hold, f must satisfy the integral equation

$$\int_0^{\infty} f(z-\zeta^2)\,d\zeta = \tfrac{1}{2}F(z).* \qquad (7)$$

* The equation should really be $\int_0^{\infty} f(z-\zeta^2)\,d\zeta = \tfrac{1}{2}F(z)+\text{const.}$, but it will be seen in the following (cf. (8)) that the constant has no effect on the result and can thus be ignored.

This can be transformed into Abel's integral equation, by putting

$$z-\zeta^2 = u, \quad d\zeta = -\frac{du}{2\sqrt{(z-u)}},$$

so that

$$\int_{-\infty}^{z} \frac{f(u)\,du}{\sqrt{(z-u)}} = F(z). \tag{7a}$$

Then, assuming that $\lim_{z=-\infty} F(z) = 0$, the solution of this integral equation is (Bocher 1909)

$$f(u) = \frac{1}{\pi}\int_{-\infty}^{u} \frac{F'(z)\,dz}{\sqrt{(u-z)}}.* \tag{8}$$

Now consider the expression

$$\Phi_1 = \tfrac{1}{2}F(ct+2\xi\eta) + \int_0^{\xi+\eta} f(ct+2\xi\eta-\zeta^2)\,d\zeta. \tag{9}$$

This is part of (5). It is easily verified that it satisfies the sound equation (3). It can be written differently. Introducing polar co-ordinates

$$x+iy = re^{i\theta}, \tag{10}$$

it is seen that

$$\xi+\eta = +\sqrt{(r+y)}, \quad (0 \leqslant \theta \leqslant \tfrac{3}{2}\pi); \qquad \xi+\eta = -\sqrt{(r+y)}, \quad (\tfrac{3}{2}\pi \leqslant \theta \leqslant 2\pi);$$

hence

$$\Phi_1 = \tfrac{1}{2}F(ct+y) + \int_0^{\sqrt{(r+y)}} f(ct+y-\zeta^2)\,d\zeta, \quad (0 \leqslant \theta \leqslant \tfrac{3}{2}\pi)$$

$$= \tfrac{1}{2}F(ct+y) - \int_0^{\sqrt{(r+y)}} f(ct+y-\zeta^2)\,d\zeta, \quad (\tfrac{3}{2}\pi \leqslant \theta \leqslant 2\pi).$$

Taking account of (7) this can be put into the form

$$\Phi_1 = \int_{\sqrt{(r+y)}}^{\infty} f(ct+y-\zeta^2)\,d\zeta + [F(ct+y)], \tag{9a}$$

where the brackets indicate that $F(ct+y)$ must be omitted when $\frac{3}{2}\pi \leqslant \theta \leqslant 2\pi$. Substituting for f from (8),

$$\int_{\sqrt{(r+y)}}^{\infty} f(ct+y-\zeta^2)\,d\zeta = \frac{1}{\pi}\int_{\sqrt{(r+y)}}^{\infty} d\zeta \int_{-\infty}^{ct+y-\zeta^2} \frac{F'(u)\,du}{\sqrt{(ct+y-\zeta^2-u)}}.$$

This is a double integral over u and ζ, extended over the area to the right of $\zeta = \sqrt{(r+y)}$, and bounded by the parabola $u = ct+y-\zeta^2$. Inverting the

* Lamb (1910) gave this solution in a footnote and utilized a different solution based on the application of a Fourier transform. (8) is more convenient in applications when f cannot be found explicitly.

order of integration and making the appropriate changes in the limits of integration,

$$\int_{\sqrt{(r+y)}}^{\infty} f(ct+y-\zeta^2)\,d\zeta = \frac{1}{\pi}\int_{-\infty}^{ct-r} F'(u)\,du \int_{\sqrt{(r+y)}}^{\sqrt{(ct-y+u)}} \frac{d\zeta}{\sqrt{(ct+y-u-\zeta^2)}}$$

$$= \frac{1}{\pi}\int_{-\infty}^{ct-r} F'(u)\left\{\tfrac{1}{2}\pi - \sin^{-1}\sqrt{\frac{r+y}{ct+y-u}}\right\}du.$$

Thus by a partial integration,

$$\int_{\sqrt{(r+y)}}^{\infty} f(ct+y-\zeta^2)\,d\zeta = \frac{\sqrt{(r+y)}}{2\pi}\int_{-\infty}^{ct-r} \frac{F(u)\,du}{(ct+y-u)\sqrt{(ct-r-u)}},$$

and hence

$$\Phi_1 = \frac{\sqrt{(r+y)}}{2\pi}\int_{-\infty}^{ct-r} \frac{F(u)\,du}{(ct+y-u)\sqrt{(ct-r-u)}} + [F(ct+y)], \tag{11}$$

which agrees with the result given by Sommerfeld (1901, p. 40).

Formulae for the pressure. Approximations

In the preceding section the solution of the problem of the diffraction of a pulse of arbitrary shape by a semi-infinite wall has been developed in terms of the velocity potential. In the following we shall be mainly concerned with the pressure, so that it is best to transcribe the solution obtained into terms of pressure. The pressure, p (i.e. the pressure in excess over that of the undisturbed atmosphere), is connected with the velocity potential by the relation

$$p = \rho\frac{\partial\Phi}{\partial t}. \tag{12}$$

Now it was found that

$$\Phi = \tfrac{1}{2}F(ct+y) + \tfrac{1}{2}F(ct-y) + \int_0^{\xi+\eta} f(ct+y-\zeta^2)\,d\zeta + \int_0^{\xi-\eta} f(ct-y-\zeta^2)\,d\zeta.$$

The function f is continuous, so that differentiation under the integral sign is permissible. Thus

$$p = \rho c\Big\{\tfrac{1}{2}F'(ct+y) + \tfrac{1}{2}F'(ct-y) + \int_0^{\xi+\eta} f'(ct+y-\zeta^2)\,d\zeta + \int_0^{\xi-\eta} f'(ct-y-\zeta^2)\,d\zeta\Big\}. \tag{13}$$

From now on we shall assume that the incident pulse has a definite wave front, so that we can put

$$F(z) = 0 \quad (z \leqslant 0). \tag{14}$$

Then the equations (7a) and (8) become

$$f(u) = \frac{1}{\pi}\int_0^u \frac{F'(z)\,dz}{\sqrt{(u-z)}}; \quad F(z) = \int_0^z \frac{f(u)\,du}{\sqrt{(z-u)}}. \tag{15}$$

To effect the differentiation of f, a partial integration is performed first. Thus it is found that

$$f(u) = \frac{1}{\pi}\int_0^u \frac{F'(z)\,dz}{\sqrt{(u-z)}} = \frac{1}{\pi}\left\{2\sqrt{u}\,F'(0) + 2\int_0^u \sqrt{(u-z)}\,F''(z)\,dz\right\},$$

hence

$$f'(u) = \frac{F'(0)}{\pi\sqrt{u}} + \frac{1}{\pi}\int_0^u \frac{F''(z)\,dz}{\sqrt{(u-z)}}, \tag{16}$$

as we cannot suppose that $F'(0) = 0$. Introducing a new auxiliary function ϕ and the pressure of the incident pulse p_0, by putting

$$\phi(u) = \rho c f'(u), \quad p_0(z) = \rho c F'(z), \tag{17}$$

the equations (13) and (16) can be written

$$\phi(u) = \frac{p_0(0)}{\pi\sqrt{u}} + \frac{1}{\pi}\int_0^u \frac{p_0'(z)\,dz}{\sqrt{(u-z)}}, \tag{16a}$$

$$p = \tfrac{1}{2}p_0(ct+y) + \tfrac{1}{2}p_0(ct-y) + \int_0^{\xi+\eta} \phi(ct+y-\zeta^2)\,d\zeta + \int_0^{\xi-\eta} \phi(ct-y-\zeta^2)\,d\zeta. \tag{13a}$$

The converse of (16a) is obtained by differentiating the second equation in (15) and introducing ϕ and p_0. Since $f(0) = 0$ it is found that

$$p_0(z) = \int_0^z \frac{\phi(u)\,du}{\sqrt{(z-u)}}. \tag{18}$$

Remembering that the transformation (1) transforms the whole of the x-y-plane into the upper half of the ξ-η-plane, and that therefore always $\eta > 0$, it is easily deduced that

$$\left.\begin{aligned}
&\text{(Region 1)}\ \xi+\eta = +\sqrt{(r+y)}, \quad \xi-\eta = +\sqrt{(r-y)}, \quad (x>0, y>0; 0<\theta<\tfrac{1}{2}\pi),\\
&\text{(Region 2)}\ \xi+\eta = +\sqrt{(r+y)}, \quad \xi-\eta = -\sqrt{(r-y)}, \quad (x<0, \tfrac{1}{2}\pi<\theta<\tfrac{3}{2}\pi),\\
&\text{(Region 3)}\ \xi+\eta = -\sqrt{(r+y)}, \quad \xi-\eta = -\sqrt{(r-y)}, \quad (x>0, y<0, \tfrac{3}{2}\pi<\theta<2\pi).
\end{aligned}\right\} \tag{19}$$

Hence making use of the equation (18), it is seen that the formula for the pressure, (13a), can be written as follows:

$$p_1 = p_0(ct+y)+p_0(ct-y)-\int_{\sqrt{(r+y)}}^{\sqrt{(ct+y)}} \phi(ct+y-\zeta^2)\,d\zeta-\int_{\sqrt{(r-y)}}^{\sqrt{(ct-y)}} \phi(ct-y-\zeta^2)\,d\zeta,$$

$$p_2 = p_0(ct+y)-\int_{\sqrt{(r+y)}}^{\sqrt{(ct+y)}} \phi(ct+y-\zeta^2)\,d\zeta+\int_{\sqrt{(r-y)}}^{\sqrt{(ct-y)}} \phi(ct-y-\zeta^2)\,d\zeta,$$

$$p_3 = \int_{\sqrt{(r+y)}}^{\sqrt{(ct+y)}} \phi(ct+y-\zeta^2)\,d\zeta+\int_{\sqrt{(r-y)}}^{\sqrt{(ct-y)}} \phi(ct-y-\zeta^2)\,d\zeta,$$

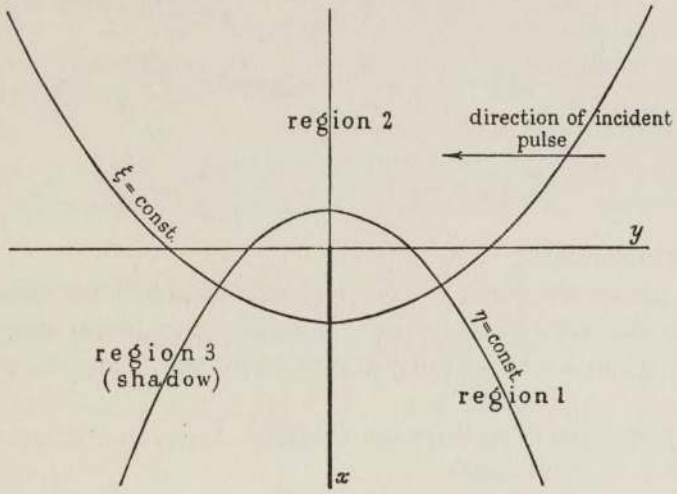

FIGURE 1

where the indices 1, 2, 3 indicate that these formulae apply in the regions labelled 1, 2, 3 in (19) (see also figure 1). Now the integrals appearing in these formulae can be transformed by the substitutions

$$ct+y-\zeta^2 = u, \quad \int_{\sqrt{(r+y)}}^{\sqrt{(ct+y)}} \phi(ct+y-\zeta^2)\,d\zeta = \frac{1}{2}\int_0^{ct-r} \frac{\phi(u)\,du}{\sqrt{(ct+y-u)}},$$

$$ct-y-\zeta^2 = u, \quad \int_{\sqrt{(r-y)}}^{\sqrt{(ct-y)}} \phi(ct-y-\zeta^2)\,d\zeta = \frac{1}{2}\int_0^{ct-r} \frac{\phi(u)\,du}{\sqrt{(ct-y-u)}}.$$

Then, introducing the function

$$P(X,T) = \int_0^T \frac{\phi(u)\,du}{\sqrt{(T+X-u)}}, \tag{20}$$

the following expressions for the pressure are obtained:

$$\left.\begin{aligned} p_1 &= p_0(ct+y)+p_0(ct-y)-\tfrac{1}{2}\{P(X_1,T)+P(X_2,T)\},\\ p_2 &= p_0(ct+y)-\tfrac{1}{2}\{P(X_1,T)-P(X_2,T)\},\\ p_3 &= \tfrac{1}{2}\{P(X_1,T)+P(X_2,T)\}, \end{aligned}\right\} \tag{21}$$

where $$X_1 = r+y, \quad X_2 = r-y, \quad T = ct-r. \tag{21a}$$

It is possible to express the function P directly in terms of p_0. For, using (16a),

$$P(X,T) = \frac{2p_0(0)}{\pi}\tan^{-1}\sqrt{\frac{T}{X}}+\frac{1}{\pi}\int_0^T p_0'(z)\,dz\int_z^T \frac{du}{\sqrt{[(u-z)(T+X-u)]}}$$

$$= \frac{2p_0(0)}{\pi}\tan^{-1}\sqrt{\frac{T}{X}}+\frac{2}{\pi}\int_0^T p_0'(z)\tan^{-1}\sqrt{\frac{T-z}{X}}\,dz,$$

hence $$P(X,T) = \frac{\sqrt{X}}{\pi}\int_0^T \frac{p_0(z)\,dz}{(T+X-z)\sqrt{(T-z)}}, \tag{20a}$$

by a partial integration.

Thus the pressure is given by (21) in terms of the incident pressure pulse p_0 and of the function P. It is useful to have approximate expressions for this function when X is either very large or very small. These can be obtained as follows:

(1) *X is very large.* The variation of $\sqrt{(T+X-u)}$ in the interval $(0, T)$ is small and so approximately

$$P(X,T) = \frac{1}{\sqrt{X}}\int_0^T \phi(u)\,du = \frac{1}{\sqrt{X}}\Psi(T). \tag{22}$$

It follows from (17) and (15) that

$$\Psi(T) = \frac{1}{\pi}\int_0^T \frac{p_0(z)\,dz}{\sqrt{(T-z)}}. \tag{23}$$

(2) *X is small.* We can write

$$P(X,T) = \int_0^{T+X}\frac{\phi(u)\,du}{\sqrt{(T+X-u)}}-\int_T^{T+X}\frac{\phi(u)\,du}{\sqrt{(T+X-u)}} = p_0(T+X)-I(X,T).$$

Then, by a partial integration,

$$I(X,T) = \int_T^{T+X}\frac{\phi(u)\,du}{\sqrt{(T+X-u)}} = 2\phi(T)\sqrt{X}+2\int_T^{T+X}\phi'(u)\sqrt{(T+X-u)}\,du.$$

An upper limit for the integral appearing after the partial integration has been performed is clearly given by

$$\left| 2\int_{T}^{T+X} \phi'(u)\sqrt{(T+X-u)}\,du \right| \leqq 2X^{\frac{3}{2}} |\,\phi'_{\max.}(T,X)\,|,$$

where $|\,\phi'_{\max.}(T,X)\,|$ is the greatest value of $|\,\phi'(T)\,|$ in the interval $(T, T+X)$; if X and $|\,\phi'_{\max.}\,|$ are sufficiently small, the integral can be neglected and thus

$$P(X,T) = p_0(T+X) - 2\sqrt{X}\,\phi(T) \text{ approximately.} \tag{24}$$

It will be seen in the following that these approximations are very useful when calculating the pressure distribution near the boundary of the 'geometrical shadow' of the wall.

It follows from approximation (22) that when X is sufficiently large, $P(X,T)$ can be neglected. It is thus possible to discuss the behaviour of the diffracted pulse far away from the edge of the wall. In terms of polar co-ordinates

$$X_1 = r(1+\sin\theta), \quad X_2 = r(1-\sin\theta).$$

Now suppose that θ varies while r is kept fixed, r being very large. Assuming that P can be neglected if $X > X^*$ it appears that the terms in P in the equations (21) can be neglected everywhere except for a certain region containing the y-axis, whose boundary will be approximately given by the parabolas

$$r(1+\sin\phi) = X^*, \quad r(1-\sin\phi) = X^*. \tag{25}$$

Outside this region

$$\left.\begin{aligned} p_1 &= p_0(ct+y) + p_0(ct-y), \\ p_2 &= p_0(ct+y), \\ p_3 &= 0. \end{aligned}\right\} \tag{26}$$

The pressure varies continuously in the area bounded by (25) and we find that on the boundary of the shadow very far from the origin,

$$\left.\begin{aligned} p &\to \tfrac{1}{2}p_0(ct+y), && (x=0,\ y\to-\infty) \\ p &\to \tfrac{1}{2}p_0(ct+y) + \tfrac{1}{2}p_0(ct-y), && (x=0,\ y\to+\infty) \end{aligned}\right\} \tag{26a}$$

since

$$P(0,T) = p_0(T).$$

Calculations: the pulse $p_0 = (1-z)\,e^{-z}$

The theoretical results developed in the preceding sections have been applied to the detailed discussion of the diffraction of a pulse given by

$$\left.\begin{aligned} p_0(ct+y) &= \left(1-\frac{ct+y}{\lambda}\right)\exp\left[-\frac{ct+y}{\lambda}\right], && (ct+y>0)\\ &= 0 && (ct+y<0)\end{aligned}\right\} \tag{27}$$

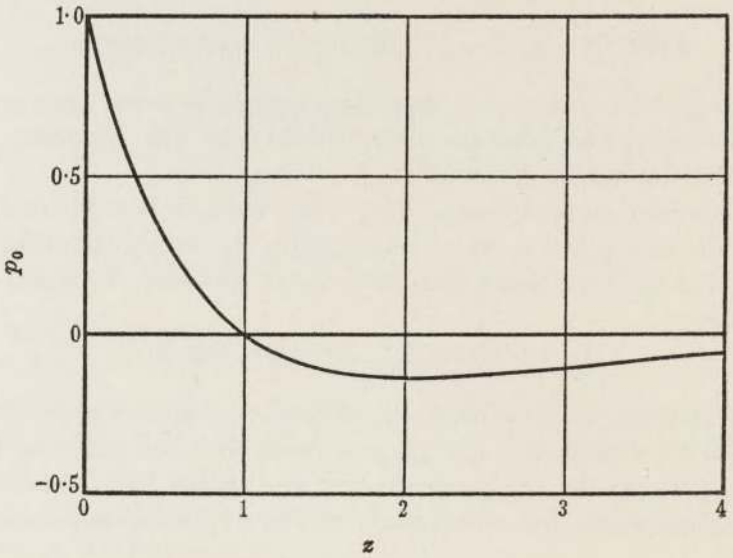

Figure 2. The pulse $p_0(z) = (1-z)\,e^{-z}$.

(see figure 2). λ is here a certain parameter characterizing the pulse which may be called the 'pulse thickness'. It is more convenient to use non-dimensional variables. We chose the pulse thickness as the unit of length, so that from now on x and y stand for x/λ, y/λ, i.e. they are the distances measured in terms of λ. The time t is replaced by the variable z which is connected with it by the relation

$$z = \frac{ct}{\lambda}. \tag{28}$$

(27) can then be rewritten as

$$\left.\begin{aligned} p_0(z+y) &= [1-(z+y)]\,e^{-(z+y)}, && (z+y>0)\\ &= 0. && (z+y<0)\end{aligned}\right\} \tag{27a}$$

The first step in the evaluation of the result is the calculation of the auxiliary functions Ψ, Ψ', Ψ''. It is found from (23) that

$$\Psi = \frac{1}{\pi}\int_0^T \frac{(1-z)\,e^{-z}}{\sqrt{(T-z)}}\,dz = \frac{2e^{-T}}{\pi}\int_0^{\sqrt{T}} (1-T+u^2)\,e^{u^2}\,du,$$

where the second form is easily obtained from the first by a change of variable. By a partial integration it is found that

$$\int_0^{\sqrt{T}} 2u^2 e^{u^2}\,du = -\int_0^{\sqrt{T}} e^{u^2}\,du + e^T\sqrt{T}.$$

Hence the following three expressions are obtained:

$$\Psi(T) = \frac{e^{-T}}{\pi}(1-2T)\int_0^{\sqrt{T}} e^{u^2}\,du + \frac{\sqrt{T}}{\pi}, \tag{29a}$$

$$\Psi'(T) = \frac{e^{-T}}{\pi}(2T-3)\int_0^{\sqrt{T}} e^{u^2}\,du + \frac{1}{\pi}\left(\frac{1}{\sqrt{T}} - \sqrt{T}\right), \tag{29b}$$

$$\Psi''(T) = \frac{e^{-T}}{\pi}(5-2T)\int_0^{\sqrt{T}} e^{u^2}\,du + \frac{1}{\pi}\left(\sqrt{T} - \frac{2}{\sqrt{T}} - \frac{1}{2T^{\frac{3}{2}}}\right). \tag{29c}$$

TABLE 1. THE FUNCTION $f(z) = (1-z)\,e^{-z}$

z	$f(z)$	z	$f(z)$	z	$f(z)$
0·00	1·000	1·25	−0·072	3·00	−0·100
0·25	0·583	1·50	−0·111	3·50	−0·075
0·50	0·303	1·75	−0·130	4·00	−0·057
0·75	0·115	2·00	−0·135	4·50	−0·039
1·00	0·000	2·50	−0·123	5·00	−0·027

TABLE 2. THE FUNCTIONS $\Psi(T)$, $\Psi'(T)$, $\Psi''(T)$ (cf. formulae (29*a*)–(29*c*))

T	$\Psi(T)$	$\Psi'(T)$	$\Psi''(T)$
0·0	0·000	∞	−∞
0·2	0·217	0·246	−1·492
0·4	0·232	−0·038	−0·777
0·6	0·212	−0·146	−0·263
0·8	0·182	−0·170	−0·066
1·0	0·147	−0·171	0·036
1·5	0·070	−0·130	0·103
2·0	0·018	−0·081	0·088
2·5	0·000	−0·051	0·062
3·0	−0·028	−0·020	0·037
3·5	−0·034	−0·006	0·022
4·0	−0·035	0·002	0·011
4·5	−0·028	0·002	0·007
5·0	−0·026	0·005	0·002

TABLE 3. DIFFRACTED PRESSURE-TIME CURVES FOR THE INCIDENT PULSE

$$p_0 = (1-z)\,e^{-z}$$

NEAR THE BOUNDARY OF THE SHADOW, AT $y = -10$

(*a*) *outside the shadow*

τ	$x=-1{\cdot}0$	$x=-0{\cdot}8$	$x=-0{\cdot}6$	$x=-0{\cdot}4$	$x=-0{\cdot}2$	$x=0{\cdot}0$
0·0	1·000	1·000	1·000	1·000	1·000	0·500
0·2	0·443	0·444	0·416	0·402	0·388	0·360
0·4	0·236	0·241	0·230	0·221	0·193	0·232
0·6	0·107	0·110	0·114	0·122	0·128	0·146
0·8	0·032	0·039	0·044	0·052	0·056	0·069
1·0	−0·023	−0·009	−0·006	0·004	0·006	0·016
1·5	−0·080	−0·072	−0·063	−0·061	−0·054	−0·048
2·0	−0·088	−0·080	−0·072	−0·073	−0·070	−0·063
2·5	−0·071	−0·070	−0·068	−0·068	−0·068	−0·060
3·0	−0·054	−0·055	−0·056	−0·057	−0·054	−0·051

(*b*) *inside the shadow*

T	$x=0{\cdot}2$	$x=0{\cdot}4$	$x=0{\cdot}6$	$x=0{\cdot}8$	$x=1{\cdot}0$
0·0	0·000	0·000	0·000	0·000	0·000
0·2	0·337	0·321	0·306	0·289	0·275
0·4	0·228	0·226	0·225	0·218	0·210
0·6	0·139	0·143	0·146	0·148	0·148
0·8	0·072	0·079	0·085	0·089	0·092
1·0	0·024	0·030	0·036	0·042	0·046
1·5	−0·042	−0·037	−0·032	−0·026	−0·022
2·0	−0·058	−0·058	−0·055	−0·051	−0·046
2·5	−0·059	−0·057	−0·054	−0·052	−0·049
3·0	−0·052	−0·051	−0·050	−0·049	−0·047

TABLE 4. PRESSURE-TIME CURVES AT VARIOUS POINTS IN THE SHADOW

(incident pulse, $p_0(z) = (1-z)\,e^{-z}$)

T	$x=0{\cdot}75$ $y=0{\cdot}00$	$x=1{\cdot}50$ $y=0{\cdot}00$	$x=1{\cdot}50$ $y=-1{\cdot}50$	$x=1{\cdot}50$ $y=-3{\cdot}00$
0·00	0·000	0·000	0·000	0·000
0·25	0·242	0·179	0·180	0·205
0·50	0·212	0·210	0·176	0·175
0·75	0·149	0·167	0·138	0·133
1·00	0·098	0·098	0·091	0·084
1·50	0·012	0·026	0·021	0·013
2·00	−0·034	−0·004	−0·017	−0·021
2·50	−0·046	−0·026	−0·030	−0·040
3·00	−0·054	−0·036	−0·031	−0·038

TABLE 5. DIFFERENCE OF THE PRESSURES ON THE TWO SIDES OF THE WALL AT TWO POINTS

(incident pulse, $p_0(z) = (1-z)\,e^{-z}$)

z	$x = 0{\cdot}75$	$x = 1{\cdot}50$
0·00	2·000	2·000
0·25	1·164	1·164
0·50	0·606	0·606
0·75	0·229	0·229
1·00	−0·484	0·000
1·50	−0·621	−0·223
2·00	−0·378	−0·710
2·50	−0·206	−0·442
3·00	−0·119	−0·251
3·50	−0·046	−0·142
4·00	−0·001	−0·063

TABLE 6. DIFFRACTED PRESSURE-TIME CURVES FOR THE INCIDENT PULSE

$p_0(z) = 0 \quad (z \leqslant 0)$; $\qquad p_0(z) = 2z \quad (0 \leqslant z \leqslant \frac{1}{2})$;

$p_0(z) = 2(1-z) \quad (\frac{1}{2} \leqslant z \leqslant 1)$; $\qquad p_0(z) = 0 \quad (z \geqslant 1)$

NEAR THE BOUNDARY OF THE SHADOW, AT $y = -10$

	(*a*) *outside the shadow*			(*b*) *inside the shadow*		
τ	$x = -1{\cdot}0$	$x = -0{\cdot}5$	$x = 0{\cdot}0$	T	$x = 0{\cdot}5$	$x = 1{\cdot}0$
0·00	0·000	0·000	0·000	0·00	0·000	0·000
0·25	0·490	0·363	0·262	0·25	0·203	0·162
0·50	0·642	0·602	0·534	0·50	0·445	0·376
0·75	0·214	0·262	0·287	0·75	0·296	0·288
1·00	−0·058	−0·010	0·027	1·00	0·072	0·105
2·00	−0·005	0·016	0·024	2·00	0·034	0·042
3·00	0·015	0·023	0·020	3·00	0·025	0·029

Tables for $\int_0^Z e^{u^2}\,du$

are available as far as $Z = 2$ (Jahnke-Emde 1933). These allow the calculation of Ψ, Ψ', Ψ'' as far as $T = 4$. For larger values of T, the integral was found by numerical integration. As great accuracy is not required over this range, the values of the functions (29) being small, this integration must be considered as a somewhat rough approximation to the exact value of the integral. The graphs of Ψ, Ψ', Ψ'' are shown in figure 3.

Figure 4 summarizes results relating to the behaviour of the pressure close to the edge of the geometrical shadow of the wall. A number of

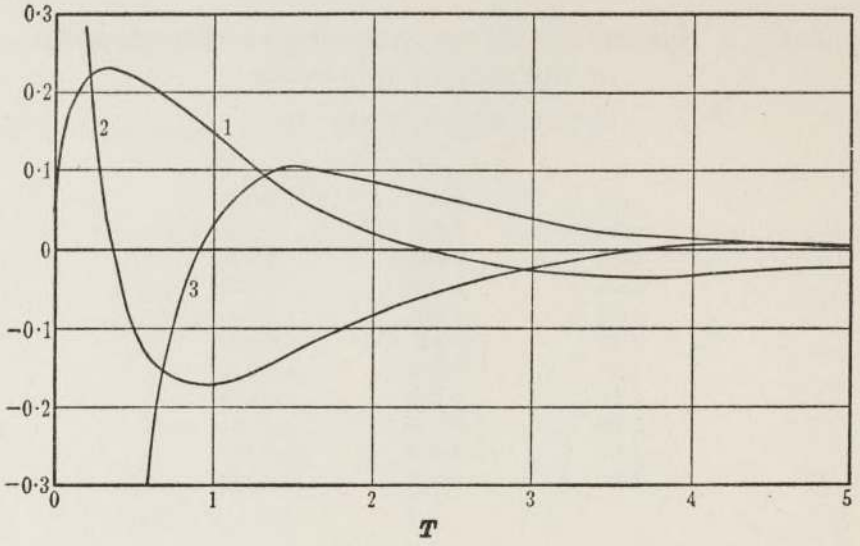

FIGURE 3. The functions Ψ, Ψ', Ψ'' for the incident pulse $p_0(z) = (1-z)\,e^{-z}$. The ordinate in curve 1 shows $\Psi(T)$, curve 2 $\Psi'(T)$, curve 3 $\Psi''(T)$.

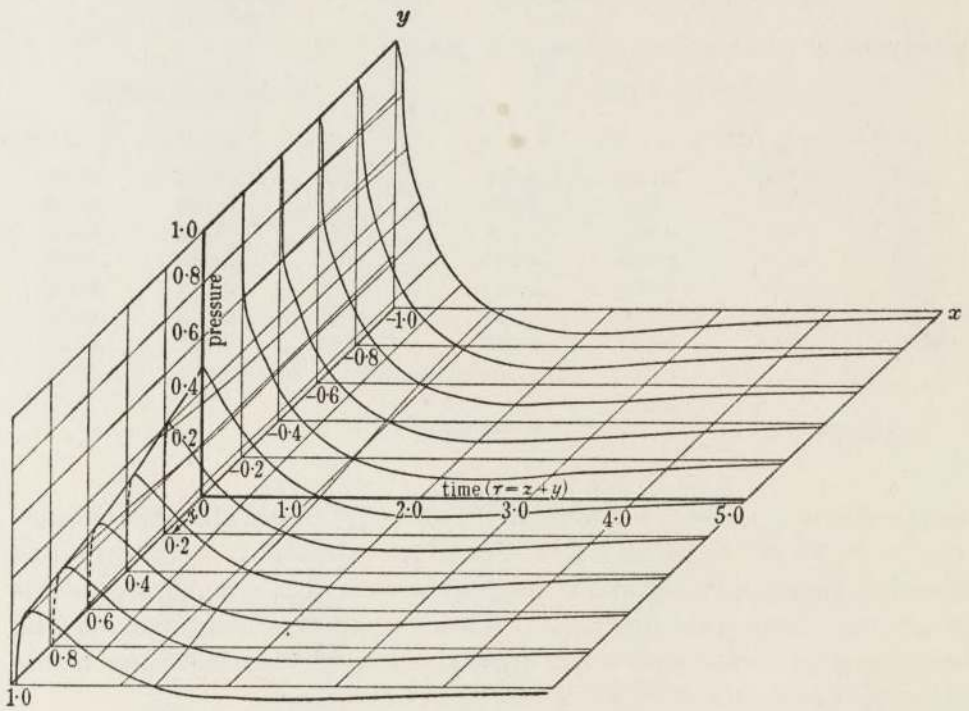

FIGURE 4. Pressure as a function of x and time at $y = -10$. The boundary of the geometrical shadow is $x = 0_+$.

pressure-time curves have been computed at points where $y = -10$, and x ranges from $+1$ to -1. These curves are superposed in the figure in such a way that they form the oblique projection of a surface whose perpendicular height represents the pressure. In the figure, the vertical ordinates represent the pressure; the horizontal ones the time; and the third co-ordinate measured parallel to the third (inclined) axis the distance from the edge of the shadow.

A remarkable feature, which will occur in all cases where a pulse with a discontinuous initial pressure rise is diffracted, is the initial pressure discontinuity across the boundary of the shadow which can be seen in the figure. The diffracted pulse consists of two components; one is a pulse with the cylindrical wave front $z = r$; the other one is, in the region under consideration, the incident pulse, which is propagated outside the shadow. Thus at any point outside the shadow the full and undistorted incident pulse will be experienced until the diffracted wave, which starts at the origin, arrives. The wave fronts touch at the boundary of the shadow; across this boundary the pressure is in general continuous, except initially. In fact, however close to the boundary a point may be, there will still be a small interval of time during which the incident pulse is experienced while the 'cylindrical' pulse has not yet arrived. If the incident pressure pulse starts discontinuously, then this discontinuity is thus propagated along the boundary of the shadow. If the pressure of the incident pulse rises continuously from the start, no discontinuity will occur at all (for an example cf. figure 9). It is evident from the nature of this phenomenon that it would not easily be detected if the solution employed were of the Fourier transform type.

Figure 4 shows clearly the attenuating effect of the wall: the maximum pressure reached falls off very quickly to about a third of the maximum pressure of the incident pulse.

The calculations were carried out by using the approximations (22) and (24) developed in the preceding section. These cannot be used to calculate the pressure immediately after the onset of the wave, however, as $\Psi'(T)$ and $\Psi''(T)$ are infinite when $T = 0$. For this purpose different approximations were obtained by replacing $(1-z)e^{-z}$ by $1-2z$. An application of $(20a)$ yields the result

$$P^*(X, T) = \frac{2}{\pi}\sqrt{(XT)} + \frac{2}{\pi}(1-2T-X)\tan^{-1}\sqrt{\frac{T}{X}}. \qquad (30)$$

The asterisk indicates that this is only an approximation. (30) was only

used for $0 \leqslant T \leqslant 0{\cdot}2$. For the range $T \geqslant 0{\cdot}4$ the approximations (22) and (24) were applied. Let

$$\tau = z + y$$

denote the time reckoned from the onset of the pulse at any point outside the shadow; then $\tau = T + X_1$. Hence if (22) and (24) are introduced in the formulae for the pressure, (21), it is found that the approximate expression for the pressure is:

in the shadow

$$p^* = \frac{1}{2}\left\{p_0(\tau) + \frac{1}{\sqrt{X_2}}\Psi(\tau - X_1) - 2\sqrt{X_1}\,\Psi'(\tau - X_1)\right\},$$

outside the shadow

$$p^* = \frac{1}{2}\left\{p_0(\tau) + \frac{1}{\sqrt{X_2}}\Psi(\tau - X_1) + 2\sqrt{X_1}\,\Psi'(\tau - X_1)\right\}. \qquad (31)$$

Two ways are now open of calculating the pressure without approximation (except that inherent in numerical integration). Either the formula (20) for P can be used in conjunction with the table of $\Psi' = \phi$, or formula (20a) may be used. The second method is more direct, but the first one has the advantage of furnishing the values of Ψ, Ψ', Ψ'' which are needed in the approximations. If it is used, the contribution due to the term $\frac{1}{\pi}\frac{1}{\sqrt{u}}$ in (29b) must be evaluated separately. It is

$$\frac{2}{\pi}\tan^{-1}\sqrt{\frac{T}{X}}. \qquad (32)$$

The contribution of the term $\pi\sqrt{u}$ to the result can also be evaluated explicitly, but it is more conveniently included in the numerical integration.†

To obtain a more general survey of the shadowing effect of the wall, lines of equal maximum pressure in the shadow were plotted. They are shown in figure 5. At any point, e.g. on the line labelled 0·2, the maximum pressure will be exactly 0·2. The 0·5 line coincides with the y-axis (boundary

† This is the method which was actually used in nearly all the calculations described in this paper. The reason is somewhat accidental; formulae (21), etc., were developed from the analysis in Lamb's paper (1910), as the solution given there was found unsuitable for numerical work. The bulk of the calculations had been completed when the connexion with Sommerfeld's work was realized and the formulae (20a) and (11) obtained. It will be found that if (20a) is used in the calculations described in this section, the integral $\int_0^Z e^{u^2}\,du$ will appear, so that Ψ, Ψ', Ψ'' could be computed.

of the shadow) from $y = -\infty$ until some point near the origin (whose position was not calculated: it is obviously quite close to the origin), where it departs from the y-axis; inside the small space bounded by the y-axis, the x-axis, and this part of the 0·5 line the maximum pressure rises from 0·5 to its value at the origin, which is 1·0. To plot the curves shown in figure 5, the maximum pressure at a network of points in the shadow was calculated by computing the pressure for a sufficiently long time interval at each point; the curves were then obtained by interpolation. The network consisted of the points

$$\begin{array}{lll} y=-20,\ x=1; & y=-10,\ x=1; & y=-5,\ x=1; \\ y=-20,\ x=2; & y=-10,\ x=2; & y=-5,\ x=2; \\ y=-20,\ x=3; & y=-10,\ x=3; & y=-5,\ x=3. \end{array}$$

These lines of equal maximum pressure all tend asymptotically to parabolas of the form $r+y = \text{const.}$ but the range of y in figure 5 is not large enough to permit a verification of this.

It appears that the maximum pressure reached falls off very quickly to about a third of its value in the pulse, but decreases considerably less rapidly afterwards.

Pressure-time curves at some points in the shadow are shown in figure 6. It will be noticed that the decrease in maximum pressure is accompanied by a lengthening of the time interval during which the pressure is positive (it must be remembered that the 'pressure' is actually the excess pressure over that of the undisturbed atmosphere). If any pressure-time curves are compared it will be found that the curve with the lower maximum intersects the time-axis farther away from the origin as the other curve.

The curves in figure 6 may be compared with those in figure 7, showing the pressure variations at points, also in the shadow, at the back of the wall itself. The general shapes of all these curves are very similar.

The pressure on the front of the wall, p_1, is connected with that on the back of the wall, p_3, by the relation

$$p_1+p_3 = 2p_0$$

which follows from (21). Hence the difference of the pressures on the two sides of the wall is at any point

$$p_1-p_3 = 2(p_0-p_3).$$

This pressure difference, for the points $x = 0{\cdot}75$ and $x = 1{\cdot}50$, is shown in figure 8. Due to the reflexion, the pressure is equal to twice the pressure

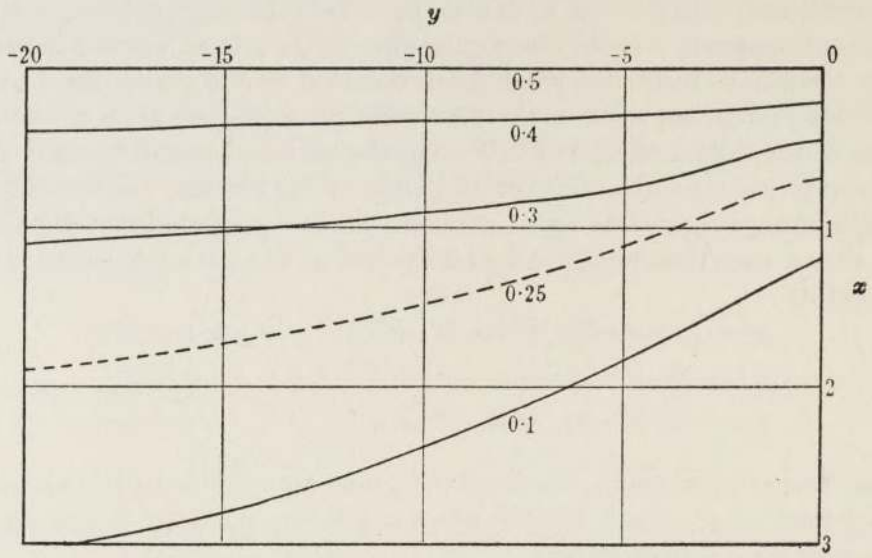

FIGURE 5. Lines of equal maximum pressure in the shadow. Note: the 0·5 line departs from the y-axis at a point near the origin.

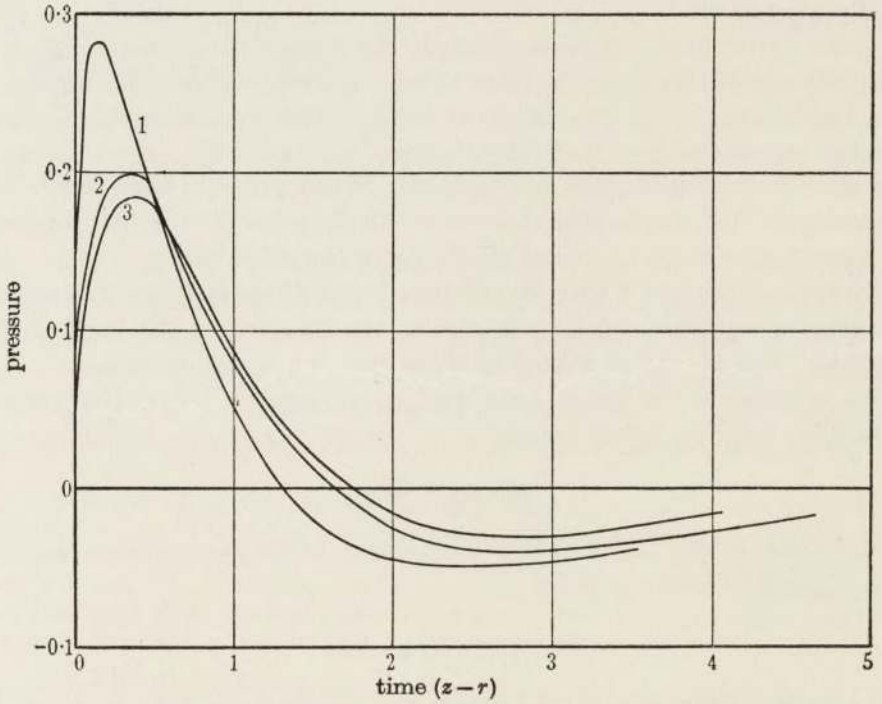

FIGURE 6. Pressure-time curves at some points in the shadow. Curve 1, $x = 1{\cdot}0$, $y = -10$; curve 2, $x = 1{\cdot}5$, $y = -3{\cdot}0$; curve 3, $x = 1{\cdot}5$, $y = -1{\cdot}5$.

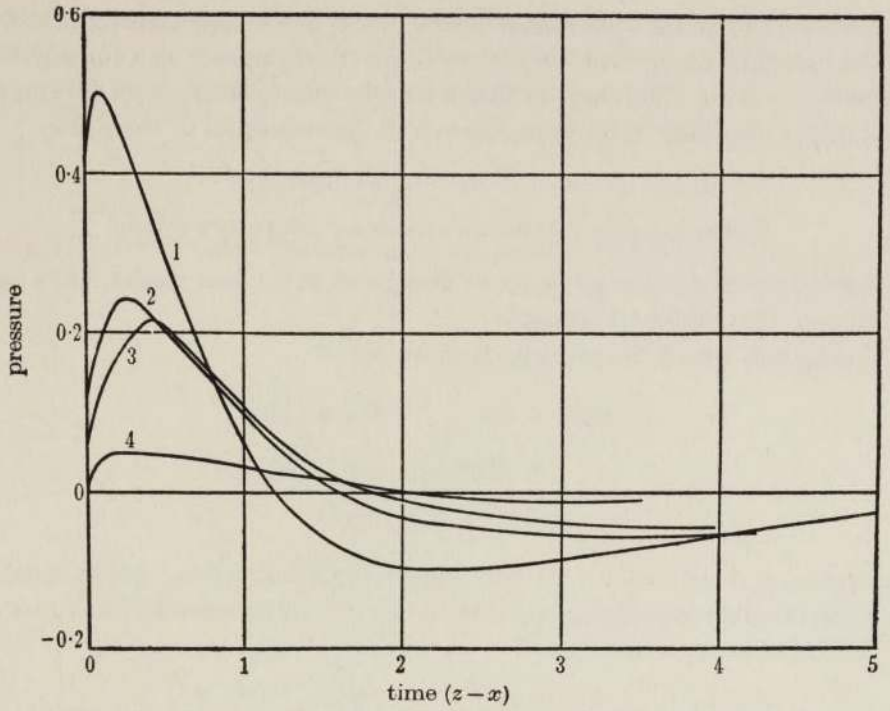

FIGURE 7. Pressure-time curves at points on the back of the wall. Curve 1, $x = 0{\cdot}05$, $y = 0$; curve 2, $x = 0{\cdot}75$, $y = 0$; curve 3, $x = 1{\cdot}5$, $y = 0$; curve 4, $x = 20$, $y = 0$.

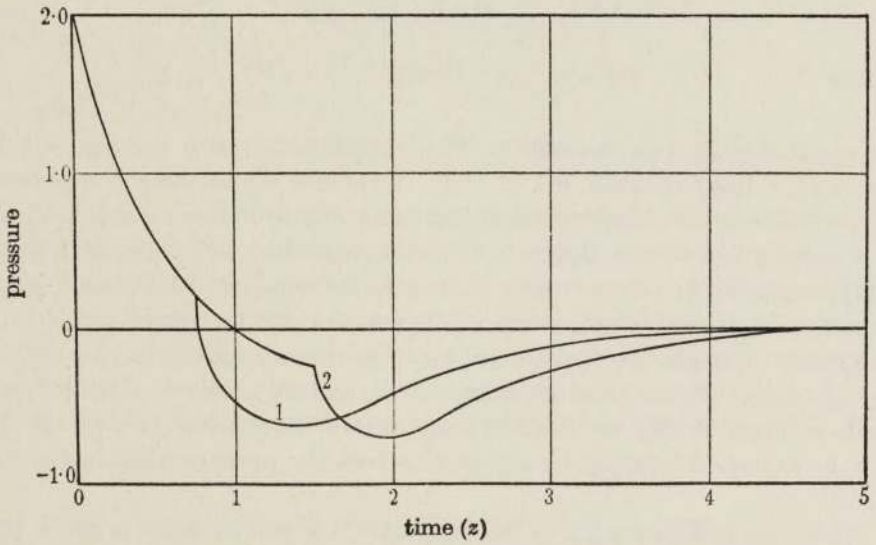

FIGURE 8. Difference of the pressures on the two sides of the wall at two points, (1) $x = 0{\cdot}75$, (2) $x = 1{\cdot}5$.

of the incident pulse until the reflected wave has arrived (simultaneously at the back and at the front of the wall); its effect appears as a considerable negative pressure difference, so that a comparatively large force acts on the wall in the direction opposite to that of the propagation of the pulse.

Calculations: various forms of incident pulse

Several other cases in addition to that given in the last section have been discussed, though less thoroughly.

For a pulse where the pressure is given by

$$\begin{aligned} p_0(z) &= 2z, && (0 \leqslant z \leqslant \tfrac{1}{2}) \\ &= 2(1-z), && (\tfrac{1}{2} \leqslant z \leqslant 1) \\ &= 0, && (z \geqslant 1) \end{aligned}$$

the pressure distribution near the edge of the shadow has been calculated in a way analogous to the discussion in the preceding section. The function $P(X, T)$ becomes in this case

$$P = X\gamma\left(\frac{T}{X}\right) \quad (0 < T \leqslant \tfrac{1}{2}), \qquad P = X\left\{\gamma\left(\frac{T}{X}\right) - 2\gamma\left(\frac{T-\frac{1}{2}}{X}\right)\right\} \quad (\tfrac{1}{2} \leqslant T \leqslant 1),$$

$$P = X\left\{\gamma\left(\frac{T}{X}\right) + \gamma\left(\frac{T-1}{X}\right) - 2\gamma\left(\frac{T-\frac{1}{2}}{X}\right)\right\} \quad (T \geqslant 1),$$

where

$$\gamma(Z) = \frac{4}{\pi}\{(1+Z)\tan^{-1}\sqrt{Z} - \sqrt{Z}\}.$$

No approximation is necessary. The calculations were carried out for $y = -10$, x ranging from -1 to $+1$. A surface whose height represents the pressure can be constructed in the same way as before, and it is shown in oblique projection in figure 9. As this pulse does not start with a discontinuous rise in pressure, the discontinuity occurring in figure 4 is not present here; the only indications of the fact that the incident pulse is being propagated outside the shadow are here the discontinuities in slope at the highest points of the pressure-time curves, and at time $\tau = 1$, outside the shadow. There is thus no marked boundary of the shadow here at all; this may be expected to apply to any pulse where the pressure rises initially at a finite rate.

When the incident pulse is 'rectangular', i.e. the pressure is given by

$$p_0(z) = 1 \quad (0 \leqslant z \leqslant 1), \qquad p_0(z) = 0 \quad (z > 1),$$

$P(X, T)$ is easily evaluated. An application of (20a) yields

$$P(X,T) = \frac{2}{\pi}\tan^{-1}\sqrt{\frac{T}{X}} \quad (T \leqslant 1)$$

$$= \frac{2}{\pi}\left(\tan^{-1}\sqrt{\frac{T}{X}} - \tan^{-1}\sqrt{\frac{T-1}{X}}\right). \quad (T \geqslant 1)$$

Some of the diffracted pressure-time curves in this case will be found in Part II of this paper.

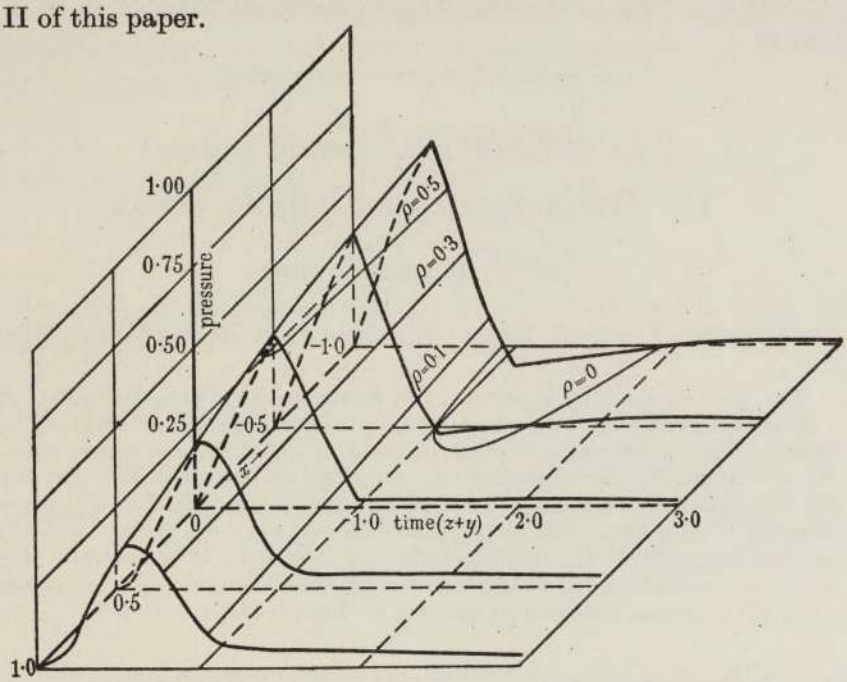

FIGURE 9. Surface $p = p(x, z)$ at $y = -10$ with level contours.

With the aid of the formulae (21), any type of incident pulse can be investigated; there is moreover no difficulty in dealing with the diffraction of a pulse whose form is only known from experiment, as it is possible to proceed by numerical integration from the start. It will be found that the case of the sharp-fronted pulse treated in the preceding section is fairly representative of a large class of pulses, viz., those which are produced suddenly and only for a short time interval. The 'rectangular pulse' is less likely to occur in practice.

In conclusion, I want to thank Professor G. I. Taylor who suggested these calculations and to whom I am indebted for much valuable advice during their progress.

REFERENCES

Bocher 1909 *Integral equations.* Camb. Math. Tracts, no. 10, p. 10.
Jahnke-Emde 1933 *Tables of Functions* (*Funktionentafeln*), 2nd ed. Leipzig, Berlin, 1933.
Lamb 1906 On Sommerfeld's diffraction problem, etc. *Proc. Lond. Math. Soc.* (2) **4**, 190.
Lamb 1910 Diffraction of a solitary wave. *Proc. Lond. Math. Soc.* (2) **8**, 422.
Sommerfeld 1895 Mathematische Theorie der Diffraktion. *Math. Ann.* **47**, 317.
Sommerfeld 1901 Theoretisches zur Beugung der Röntgenstrahlen. *Z. Math. phys.* **46**, 11.

The diffraction of sound pulses
II. Diffraction by an infinite wedge

BY F. G. FRIEDLANDER

(*Communicated by G. I. Taylor, F.R.S.—Received 29 February* 1940)

This part is a report on some calculations of the diffraction effects of infinite wedges which were carried out by means of a solution obtained by Sommerfeld. In all cases but one the incident pressure pulse was taken to be 'rectangular', i.e. to consist of unit pressure rise persisting for unit time; in one case a certain pulse discussed in detail in Part I of this paper was taken. It is found that the pressure at the summit of a wedge is actually greater than that of the incident pulse, but dies down in the shadow. The general character of the diffracted pressure-time curves is very similar to that of the curves obtained in the case of the half-plane.

In Part I of this paper the diffraction of plane sound pulses by a semi-infinite plane has been discussed. For purposes of comparison, some calculations have been made of the diffraction effect of an infinite wedge. The solution of this problem has been given by Sommerfeld (1901), but without any numerical application. The pressure-time curves were calculated for points on the back face of certain wedges, mainly in the case where the incident pulse is of the 'rectangular' type. The pressure at the summit of a wedge is actually bigger than the incident pressure, and in consequence it is found that the attenuation of the pressure due to a wedge is not as large as that due to a half-plane, while the shapes of the curves are very similar. In one case, the incident pulse has been taken as

$$p_0(z) = (1-z)\,e^{-z}, \quad (z>0)$$

a case which is discussed in detail in Part I for the half-plane.